

# Optical Induction of 2D and 3D Photonic Lattices in Photorefractive Materials based on Talbot effect

A. Badalyan, R. Hovsepyan, V. Mekhitarian, P. Mantashyan and R. Drampyan

**Abstract**—In this paper we report the technique of optical induction of 2 and 3-dimensional (2D and 3D) photonic lattices in photorefractive materials based on diffraction grating self replication -Talbot effect. 1D and 2D different rotational symmetry diffraction masks with the periods of few tens micrometers and 532 nm cw laser beam were used in the experiments to form an intensity modulated light beam profile. A few hundred micrometric scale replications of mask generated intensity structures along the beam propagation axis were observed. Up to 20 high contrast replications were detected for 1D annular mask with 30  $\mu\text{m}$  radial period. The spatial modulated intensity pattern from this mask was imparted into the lithium niobate crystal via electro-optic effect, thus creating refractive index lattice. The recorded lattices were tested by phase microscope. The spatial frequency doubling of the recorded lattice due to fractional Talbot effect was observed in the depth scanned phase microscope images.

**Keywords**—Diffraction gratings, laser, photonic lattice, Talbot effect.

## I. INTRODUCTION

ARTIFICIAL micro- and nano-structured dielectric materials [1-4], such as photonic crystals, have a great potential for numerous applications in advanced photonics and nonlinear optics [5-11]. There are different methods for the fabrication of artificial periodic structures, including etching processes, electronic beam and deep ultraviolet lithography in high refractive index materials [2-4]. Holographic technique is one of the simple and promising methods for the fabrication of spatially periodic photonic lattices in photorefractive materials [12].

The computer generated hologram and mask techniques [13] open new possibilities for formation of two-dimensional (2D) modulated light intensity profiles and recording of these intensity distributions in photosensitive materials, thus creating 2D refractive lattices. 2D photonic lattices are promising as guiding and trapping systems and for different optical devices. However, the higher three-dimensional (3D) volume photonic lattices are of great interest for high capacity optical storage, optical computers, optical communication etc. From this point of view, in spite of many successes in this field, the elaboration and realization of new methods for

optical formation of 3D photonic lattices is an actual problem. Recently Bessel standing wave technique [14] and combined interferometric-mask method [15] were suggested and realized for the creation of 2D and 3D photonic lattices in photorefractive materials.

The Talbot effect is a near field diffraction effect the essence of which is the self replication of the diffraction grating image away from the grating at regular distances (Talbot length), equaled to  $Z_T = d^2/\lambda$ , where  $d$  is the period of the grating and  $\lambda$  is wavelength of the light incident on the grating [16]. One of the interesting features of Talbot effect is the fractional revivals of the gratings, when at fractional Talbot distances sub-images can also be observed. The Talbot effect easily can be observed by one-dimensional (1D) rule diffraction gratings. In spite of the Talbot effect was discovered over than 150 years ago [17] and explained by Lord Rayleigh in 1881 [18], now it is finding the renewed interest for the formation of volume photonic lattices. The complete theory of Talbot effect is given in [19] and various applications of Talbot effect both for photonics and atom optics were discussed and realized in different works (see, for example [20- 26] and references therein).

Obviously, Talbot effect is very promising for the creation of 2D and 3D photonic lattices with the use of lower dimensional 1D and 2D transverse gratings, due to Talbot self-replication effect in the axial direction. Moreover, the exciting feature of Talbot effect to produce smaller fractional revivals of the gratings opens new possibilities for potential applications. Particularly, at half Talbot distance the replications of the grating image with half of spatial grating period take place. This opens a way for construction of nano-scale photonic lattices with the use of micrometric scale gratings.

In this paper we report the technique of optical induction of 2D and 3D periodic lattices in photorefractive materials based on rotational symmetry diffraction grating Talbot self replications. 1D and 2D different rotational symmetry diffraction masks with the periods of few tens micrometers were prepared and 532 nm cw laser beam was used in experiments to form an intensity modulated light beam profile. The interferometric testing of the prepared masks was performed. Talbot effect from 2D 6- fold symmetry and 1D annular masks were observed. The spatial modulated intensity pattern from 1D annular mask with 100 circles and 30  $\mu\text{m}$  radial period was imparted into the lithium niobate crystal via

Authors are with the Institute for Physical Research of National Academy of Sciences of Armenia, Ashtarak-2, 0203 Ashtarak, Armenia (phone: 37410 288 150; fax: 374232 31172; R.Drampyan's e-mail: rdramp@ipr.sci.am. P.Mantashyan's e-mail: paytsar.mantashyan@gmail.com

electro-optic effect, thus creating refractive index lattice. The recorded lattice was tested by phase microscope. The spatial frequency doubling of the recorded lattice due to fractional Talbot effect was observed in the depth scanned phase microscope images.

## II. OBSERVATION OF TALBOT EFFECT FROM ROTATIONAL SYMMETRY MASKS

### A. Preparation of rotational symmetry masks and testing

From 1 to 10 - fold axial symmetry masks were generated by computer graphic technique. The masks consisted of transparent holes periodically disposed along the equidistantly positioned concentric circles, surrounding the central hole. The number of the holes on the  $i$  th circle was equaled  $M_i = j \cdot i$ , where  $i = 1, 2, 3, \dots$  is integer and  $j$  is the symmetry order of the mask. The masks of reduced size (0.6 cm in diameter) with  $i = 100$  were printed by high resolution printer (3300 dpi) on the transparent film. Both the positive and negative masks were prepared.

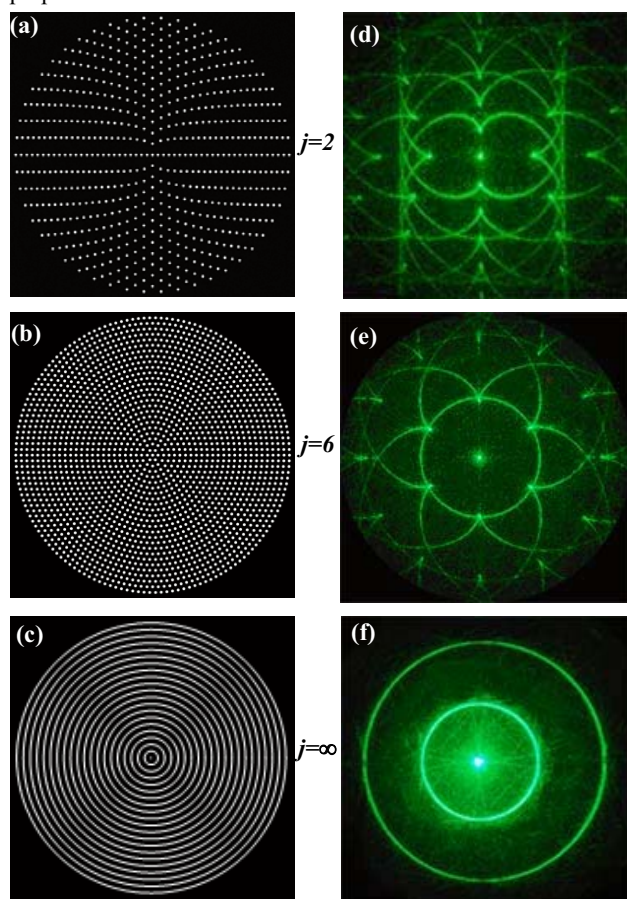


Fig. 1 (color online). (a-c) Fragments of enlarged patterns of negative 2- and 6- fold and infinite symmetry masks. The 2- and 6- fold symmetry masks had a diameter of 0.6 cm and a distance around 10-40  $\mu\text{m}$  between  $\sim 10 \mu\text{m}$  holes. The annular mask had a distance of 30  $\mu\text{m}$  between circles. (d-f) Corresponding diffraction patterns obtained in the far field from the negative 2 and 6-fold and infinite symmetry masks (a-c) by green 532 nm laser beam

The prepared negative masks had 10-60  $\mu\text{m}$  distances between 10  $\mu\text{m}$  transparent holes located on the opaque disk. The whole mask consisted of  $\sim 35000$  holes disposed along the 100 hypothetical concentric circles. Fig.1 a-c shows the fragments of 2 and 6-fold and infinite symmetry negative masks used in the present experiment. Fig.1b shows nearly equidistant 25  $\mu\text{m}$  disposition of holes in radial and azimuthal directions for 6-fold symmetry (6-fS) mask. The annular mask (Fig. 1c) is two dimensional as a pattern, but 1-dimensional as a grating with the period of 30  $\mu\text{m}$  between circles.

The masks were tested by observing the diffraction patterns from the masks in the far field by 532 nm green laser beam. The obtained high contrast diffraction patterns (Fig.1, d-f) confirm the high quality of the prepared masks.

### B. Experimental arrangement for observation of Talbot effect and results

Experimental arrangement for observation of Talbot replications of the rotational symmetry masks and measurement of Talbot distances is shown in Fig.2. The laser source was single-mode second harmonic of cw YAG:Nd laser at 532 nm wavelength with linear polarization, 100 mW power and 0.7 mm beam diameter. The profile of the green 532 nm Gaussian beam is shown in the inset of Fig. 2. The laser beam was expanded by confocal lenses and illuminated the mask. The mask plane was imaged on the CCD camera by microscope objective.

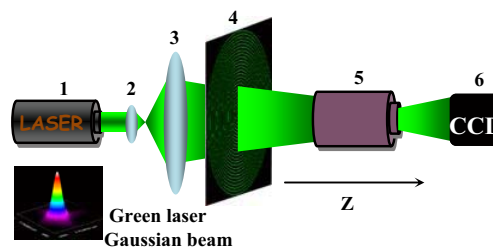


Fig. 2 (color online). Experimental set-up. 1 - laser operating at 532 nm wavelength with radiation power of 100 mW. 2, 3 - confocal lenses, 4 - mask, 5 - microscope, 6 - CCD camera

The mask was placed on the table with the possibility of micrometric scale moving along the Z axis. As the mask was moved out of the focal plane, the mask image reappeared at Talbot distances. The micrometric moving of the mask allowed the measuring of the Talbot distances with accuracy of 5  $\mu\text{m}$ .

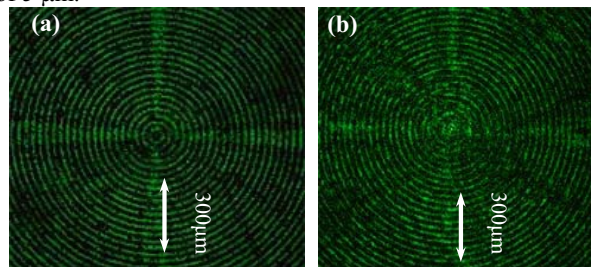


Fig.3 (color online). Self replication of circular mask at different Talbot distances: (a)  $Z_T = 0$  and (b)  $20Z_T = 31.40 \pm 0.01$  mm.

Fig.3a, b show the images of negative circular mask with the period of  $d = 30 \mu\text{m}$  at  $Z=0$ , as well as 20th self replications, respectively. The Talbot distance was measured  $Z_T = 1,57 \pm 0,01 \text{ mm}$ . The 20th self replication still shows high contrast of replicated mask image. Fig.4 shows the spatial frequency  $1/d$  doubling of the recorded lattice due to fractional Talbot effect recorded at the distance of  $Z_T/2 = 0.78 \pm 0,01 \text{ mm}$ .

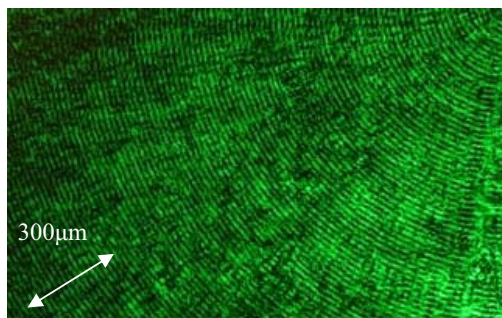


Fig.4 (color online). Self replication of circular mask at half Talbot distance:  $Z_T/2 = 0.78 \pm 0,01 \text{ mm}$

Fig.5 a, b shows the Talbot effect for 6-fS mask. The shown in Fig. 5a is the mask pattern at  $Z_T = 0$ . Fig.5b shows the lattice spatial frequency doubling at  $Z_T = 175 \pm 5 \mu\text{m}$ .

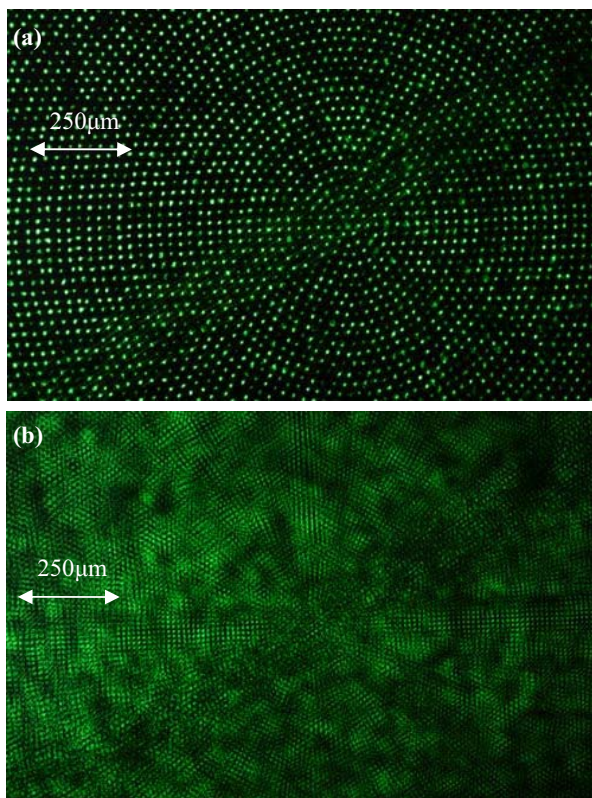


Fig.5 (color online) (a) Talbot effect from 6-fS mask at the distances  $Z_T=0$  and (b) spatial frequency doubling of lattice at  $Z_T=175 \pm 5 \mu\text{m}$

Since the 6-fS mask holes disposed nearly equidistantly in radial and azimuthal directions in the transverse plane, the

frequency doubling takes place equally for radial and azimuthal directions.

### III. RECORDING OF PHOTONIC LATTICE IN PHOTOREFRACTIVE LITHIUM NIOBATE CRYSTAL

#### A. Experimental arrangement

The recording of photonic lattice based on Talbot effect is performed in Fe doped lithium niobate (LN:Fe) crystals taking into account their large photorefractive properties and possibility of creating the long-live photonic lattices for applications. The experimental arrangement for recording of photonic lattice is shown in Fig.6. The single-mode laser beam at 532 nm wavelength with linear polarization, 100 mW power and 0.7 mm beam diameter was expanded by confocal lenses and after passing through the mask illuminated the crystal. The mask was in touch with the crystal. The optical C-axis of the crystal was oriented along the crystal surface and the polarization of laser beam was directed along the C-axis of the crystal. LN crystal doped with 0,05wt% Fe had the dimensions  $15\text{mm} \times 10\text{mm} \times 1.5 \text{ mm}$ . The annular mask was used for recording of photonic lattices in LN:Fe crystal and demonstration of the Talbot replication and frequency doubling of the recorded lattice. The duration of recording was 60 minutes.

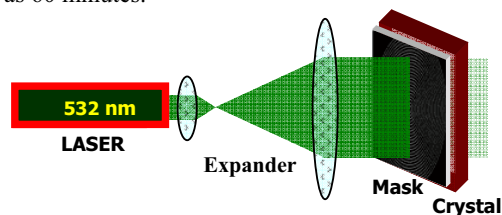


Fig.6 (color online) Experimental setup for photonic lattices recording in LN:Fe crystal.

#### B. Testing of recorded photonic lattices by phase microscope

The photonic lattices recorded in LN:Fe crystal were tested by phase microscope.

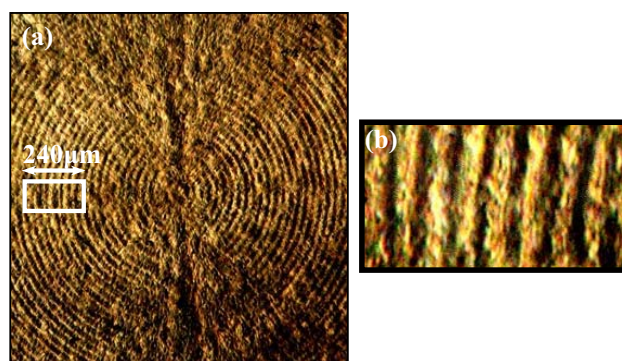


Fig.7 (Color online) Phase microscope image of photonic lattices recorded inside the LN:Fe crystal by annular mask: (a) replicated image at the exit surface of the crystal. (b) Enlarged image of the region marked by white rectangle in (a)

Fig.7,8 show the phase microscope depth scan images of recorded photonic lattice. The replicated image of the circular lattice near the exit surface of the 2mm thick crystal is shown in Fig.7. The spatial frequency doubling of the recorded lattice due to fractional Talbot effect was detected by scanning the observation plane to  $Z_T/2 = d^2/2(\lambda/n_e)$  (where  $n_e = 2.21$  is the extraordinary refractive index for LN) toward the input face of the crystal (Fig.8).

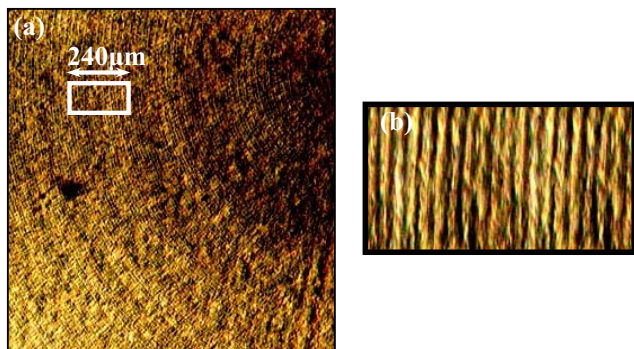


Fig.8 (Color online) Phase microscope images of photonic lattices recorded inside the LN:Fe crystal by annular mask: (a) the frequency doubled image at  $Z_T/2$  toward the input face of the crystal. (b) Enlarged image of the region marked by white rectangle in (a)

The used microscope (Union Versamet-2) did not allow the high accuracy measurements of crystal displacement during depth scan. However, such measurements will allow the measuring of refractive index of the medium by comparison of high accuracy measurements of Talbot distance of mask replication in air space and in the medium.

#### C. Physical mechanism of recording of photonic lattice in LN:Fe crystal

The physical mechanism of the formation of photonic lattices in photorefractive LN: Fe crystal is based on the electro-optic effect [27-29]. Fe ions occur in LN crystal in different valence states:  $Fe^{2+}$  and  $Fe^{3+}$ . The green light excites the electrons from  $Fe^{2+}$  to conduction band. Electrons migrate in the conduction band and finally are trapped by  $Fe^{3+}$ .

The redistribution of the charges builds up an internal electric field  $E$  and so changes the refractive index  $\Delta n_i = r_{ij}E_j$ , where  $r_{ij}$  is the electro-optic coefficient. Thus, the inhomogeneous illumination of photorefractive materials leads to the modulation of refractive index. Two main mechanisms – photovoltaic effect and diffusion of photo-induced carriers are responsible for the formation of refractive lattices in photorefractive crystal [27-29.] The diffusion effect can be neglected for lattice spatial frequencies less than  $10^5$  lines/cm [28] which is in case of the present experiment. The electric field induced by photovoltaic effect is due to the charge separation taking place along the C-axis of the crystal [28]. Induced electric field is determined by  $E_{pV} = \alpha k I / \sigma$  where  $\alpha$  is the absorption coefficient,  $k$  is the Glass constant depending on the nature of absorbing centers and light wavelength,  $I$  is the light intensity,  $\sigma$  is conductivity of the illuminated part of the crystal [28]. In Fe doped LN crystal the

change of extraordinary refractive index is larger than the change of ordinary index by a factor of four [29] and the induced refractive index change  $\Delta n$  is mainly due to the distortion of the extraordinary index of refraction  $n_e$ .

#### IV. CONCLUSION

The technique of optical induction of 2D and 3D periodic lattices in photorefractive materials based on rotational symmetry diffraction masks Talbot self replications was studied experimentally. 1D and 2D different rotational symmetry diffraction masks with the periods of few tens micrometers were prepared and 532 nm cw laser beam was used in the experiments to form an intensity modulated light beam profile. The interferometric testing of prepared masks was performed and showed their high quality. Talbot effect from 2D 6-fold symmetry masks and 1D annular mask were observed. The spatial modulated intensity pattern from 1D annular mask with 100 circles and 30  $\mu m$  radial period was imparted into the lithium niobate crystal via electro-optic effect, thus creating refractive index lattice. The recorded lattice was tested by phase microscope. The spatial frequency doubling of the recorded lattice due to fractional Talbot effect was observed in the depth scanned phase microscope images. The physical mechanism of recording of photonic lattices in photorefractive LN:Fe crystal is discussed.

The observations of Talbot self-replications from 2-fold rotational symmetry mask shown in Fig.1a seem more interesting. Since the period of this mask is different along the X and Y- directions one can expect the different fractional replications for different parts of the mask at the same Talbot distance. These experiments are in progress and will be reported elsewhere.

#### ACKNOWLEDGMENT

This work is supported by International Science and Technology Center Grant, Project A-1517.

#### REFERENCES

- [1] E. Yablonovitch, "Inhibited spontaneous emission in solid-state physics and electronics," *Phys. Rev. Lett.*, vol. 58, pp. 2059-2062, May 1987.
- [2] J. Joannopoulos, S. Johnson, R. Meade, J. Winn, *Photonic crystals*, Princeton Univ. Press. 2008.
- [3] S. Arishmar Cerqueira Jr, "Recent progress and novel applications of photonic crystal fibers," *Rep. Prog. Phys.*, vol. 73, no. 2, pp. 024401 (1-21), February 2010.
- [4] T. F. Krauss, R. M. De La Rue, "Photonic crystals in the optical regime – past, present and future," *Progress in Quantum Electronics*, vol. 23, no. 2, pp. 51-96, March 1999.
- [5] A. Arie, G. Rosenman, A. Korenfeld A. Skiliar, M. Oron, D. Eger, "Efficient resonant frequency doubling of a cw Nd:YAG laser in bulk periodically poled KTiOPO<sub>4</sub>," *Opt. Lett.*, vol. 23, no. 1, pp. 28-30, January 1998.
- [6] T. Kartaloglu, K. G. Korpulu, O. Aytur, M. Suidheimer, W. R. Risk, "Femtosecond optical parametric oscillator based on periodically poled KTiOPO<sub>4</sub>," *Opt. Lett.*, vol. 23, no.1, pp. 61-63, January 1998.
- [7] M. Ebrahimzadeh, G. A. Turnbull, T. J. Edwards, D. J. M. Stothard, I. D. Lindsay, M. H. Dunn, "Intracavity continuous-wave singly resonant optical parametric oscillators," *JOSA B*, vol. 16, no. 9, pp.1499-1511, September 1999.

- [8] D. Kasimov, A. Arie, E. Winbrand, G. Rosenman, A. Bruner, P. Shaier, D. Eger, "Annular symmetry nonlinear frequency converters," *Opt. Express*, vol. 20, no. 20, pp. 9371-9376, October 2006.
- [9] S. M. Saltiel, D. N. Neshev, R. Fischer, W. Krolikowski, A. Arie, Yu. S. Kivshar, "Generation of second harmonic Bessel beams by transverse phase matching in annular periodically poled structures," *Jap. Journal Appl. Phys.*, vol. 47, no. 8, pp. 6777-6783, August 2008.
- [10] N. Voloch, T. Ellenbogen, A. Arie, "Radially symmetric nonlinear photonic crystals," *JOSA B*, vol. 26, no. 1, pp. 42-49, January 2009.
- [11] S. M. Saltiel, D. N. Neshev, W. Krolikowski, N. Voloch-Bloch, A. Arie, O. Bang, Yu .S. Kivshar, "Nonlinear diffraction from a virtual beam," *Phys. Rev. Lett.*, vol. 104, no.8, 083902-4, February 2010.
- [12] R. J. Collier, Ch. B. Buckhard, L. H. Lin, *Optical holography*, Academic press, New York, 1971.
- [13] Wai-Hon Lee, "Computer generated holograms: Techniques and applications," in *Progress in Optics*, vol. 16, chapter 3, Editor E. Wolf, North-Holland, 1978, pp. 121-232.
- [14] A. Badalyan, R. Hovsepian, V. Mekhitarian, P. Mantashyan, R. Drampyan, "New holographic method for formation of 2D gratings in photorefractive materials by Bessel standing wave," in *Fundamentals of Laser Assisted Micro- and Nanotechnologies.*, edited by Vadim P. Veiko, T. A. Vartanyan, *Proc. of SPIE* , Vol. 7996 (SPIE Bellingham, WA, 2011) 799611-1-9.
- [15] A. Badalyan, R. Hovsepian, V. Mekhitarian, P. Mantashyan, R. Drampyan, "Combined interferometric-mask method for creation of micro- and sub-micrometric scale 3D structures in photorefractive materials", in *Int. Conference on Laser Physics 2010*, edited by A. V. Papoyan, *Proc. of SPIE* Vol.7998 (SPIE Bellingham, WA, 2011) 7998OH-1-10.
- [16] K. Paturski, "The self-imaging phenomenon and its applications," in *Progress in Optics*, vol. 27, E. Wolf, Elsevier, Amsterdam, 1989, pp. 1-108.
- [17] H. F. Talbot, "Facts relating to optical science," *Phil. Mag.*, vol. 9, pp. 401-407, December 1836.
- [18] Lord Rayleigh, "On copying-diffraction gratings and some phenomena connected therewith," *Phil. Mag.*, vol. 11, no.4, pp.196-205, December 1881.
- [19] J. T. Wintrop, C. R. Worthington, "Theory of Fresnel images. I Plane periodic objects in monochromatic light," *J. Opt. Soc. Am.*, vol. 55, no. 4, pp. 373- 381, April 1965.
- [20] M. V. Berry, S. Klein, "Integer, fractional and fractal Talbot effect," *J. Mod. Optics*, vol. 43, no. 10, pp. 2139-2164, March 1996.
- [21] M. Berry, I. Marzoli, W. Shleich, "Quantum carpets, carpets of light," *Physics World*, pp. 39-44, June 2001.
- [22] N. Guerneau, B. Harchaoui, J. Primot, K. Heggarty, "Generation of achromatic and propagation invariant spot arrays by use of continuous self-imaging gratings," *Opt. Lett.*, vol. 26, no.7, pp. 411-413, April 2001.
- [23] M. Testorf, Th. J. Suleski, Yi-Chen Chuang, "Design of Talbot array illuminators for three-dimensional intensity distributions," *Opt. Express*, vol. 24, no.17, pp.7623- 7629, August 2006.
- [24] J. Courtial, G. Whyte, Z. Bouchal, J. Wagner, "Iterative algorithm for holographic shaping of non-diffracting and self-imaging light beams," *Opt. Express*, vol. 14, pp. 2108- 2116, March 2006.
- [25] Y. Chnag, J. Wen, S. N. Zu, M. Xiao, "Nonlinear Talbot effect," *Phys.Rev. Lett.*, vol.104, no.18, pp. 183901-1-4, May 2010.
- [26] C. Denz, M. Schwab, C. Weilmann, *Transverse-pattern formation in photorefractive optics*. Springer, 2003.
- [27] A. Adibi, K. Buse, D. Psaltis, "The role of carrier mobility in holographic recording in LiNbO<sub>3</sub>," *Appl. Phys. B*, vol. 72, pp. 653-659, April 2001.
- [28] A. M. Glass, D. von der Linde, T. J. Negran, "High-voltage bulk photovoltaic effect and the photorefractive process in LiNbO<sub>3</sub>," *Appl. Phys. Lett.*, vol. 25, no. 4, pp. 233-235, August 1974.
- [29] G. T. Avanesyan, E. S. Vartanyan, R. S. Mikaelyan, R. K. Hovsepian, A. R. Pogosyan, "Mechanisms of photochromic and photorefractive effects in doubly doped lithium niobate crystal," *Phys. Stat. Sol. (a)*, vol. 126, pp. 245 - 252, February. 1991.